**Journal of Al-Turath University College (JATUC)**
Open Access Journal
ISSN : 2074-5621
https://jatuc.uoturath.edu.iq/

# Detection of Lung Affected by the COVID-19 Using New CNN Architecture

**Hani Saeed Hasaan***

***Middle Technical University, Technical Engineering College of Artificial Intelligence, Baghdad, Iraq.***

**Correspondence email*: hani_saeed@mtu.edu.iq

**KEYWORDS**

X-ray scan, COVID-1, CNN, Deep-learning, chest

**ABSTRACT**

Accurate and early detection of COVID-19-related lung infection is crucial for effective clinical decision-making. This paper presents a novel four-stage convolutional neural network (4CNN) architecture for classifying chest X-ray images into three clinically consistent categories: COVID-19 infected, non-COVID abnormal, and normal lungs. The proposed model addresses dataset imbalance using class-weighted learning and evaluates performance using comprehensive medical metrics. Experimental results demonstrate strong classification performance with an overall accuracy of 92% and improved sensitivity for minority classes. 4CNN architecture is employed to provide visual explainability.

**الكلمات المفتاحية**

فيروس كوفيد-19, لشبكة عصبية التفافية رباعية المراحل, رئة, التعلّم الموزون للفئات, الكشف الدقيق والمبكر

**الملخص**

يُعدّ الكشف الدقيق والمبكر عن عدوى الرئة المرتبطة بفيروس كوفيد-19 أمرًا بالغ الأهمية لاتخاذ قرارات سريرية فعّالة. تُقدّم هذه الورقة البحثية بنيةً جديدةً لشبكة عصبية التفافية رباعية المراحل (4CNN ) لتصنيف صور الأشعة السينية للصدر إلى ثلاث فئات متسقة سريريًا: رئة مصابة بكوفيد-19، ورئة غير مصابة بكوفيد-19، ورئة سليمة. يعالج النموذج المقترح عدم توازن مجموعة البيانات باستخدام التعلّم الموزون للفئات، ويُقيّم الأداء باستخدام مقاييس طبية شاملة. تُظهر النتائج التجريبية أداءً تصنيفيًا قويًا بدقة إجمالية تبلغ 92% وحساسية محسّنة للفئات الأقل شيوعًا. تُستخدم بنية CNN 4 لتوفير تفسير مرئي.

## 1. INTRODUCTION

The COVID-19 pandemic has created an urgent need for reliable diagnostic tools. Chest X-ray imaging provides a rapid and accessible method for assessing lung involvement. Deep learning-based analysis has shown significant promise, yet challenges remain in terms of data imbalance, evaluation rigor, and explainability. Coronavirus produces lung aggravation and injuries, which can be identified effectively by chest images and registered tomography images, which are effective at recognizing Coronavirus patients from those with other lung problems [1]. Worldwide catastrophes unite individuals and spike advancements. The ongoing pandemic and the overall unfortunate results ought to present a valuable chance to push forward innovative arrangements that work with regular daily existence [2]. Coronavirus is a dangerous, infectious illness that has turned into a pandemic. The infection has developed inside the lower respiratory tract, where primary symptoms such as a cough, increasing body temperature, and chest pain start, which might develop afterward into pneumonia [3]. In the fight against Coronavirus, patients should be precisely and immediately analyzed to get legitimate clinical treatment and cut off the pandemic [4,5]. Several clinical symptoms of lung involvement vary in unaffected by COVID-19, normal, and affected by COVID-19 patients, where X-ray plays a key role in diagnosis [6,7]. For Coronavirus determination, it is basic to comprehend and classify medical images of the chest [8]. However, conventional neural network *(CNN)* categorization algorithms produce less dependable and explainable findings [9]. Supporting global efforts is essential to combat this disease. In this battle, human-made thinking is in vogue, offering a variety of important learning methods for the robotization of coronavirus recognition. CNN deep learning models have become one of the best tools for detecting coronavirus evidence by

analyzing X-ray medical images [10,11]. The clinical picture has recently been revealed that the field of health services has a huge potential for computer thinking and artificial intelligence [12]. These methods use deep learning CNNs, which are a mimic of the brain network designed specifically for pixel information processing in image recognition and processing [13,14,15]. This study proposes a novel 4CNN architecture to address these limitations. The contributions include a multi-stage CNN design, balanced training strategy, comprehensive evaluation metrics, and visual explainability. The pre-processing is done by removing unwanted regions, and three CNN layers are used to construct the framework for the medical X-ray image. The three phases of the proposed model start with the pre-processing of medical X-ray images, followed by the preparation of the pre-processed images, and finally, the approval of the model for concealed occurrences, which are not vaccinated, unaffected, or vaccinated. The rest of this document is arranged as follows: Section 2 shows a summary of the related works. Section 3 sets out in detail the proposed strategy and describes it. Section 4 presents the experimental results. Section 5 concludes the work and proposes alternative approaches for further research.

## 2. RELATED WORK

Since the COVID-19 outbreak, there has been much research utilizing X-ray images for virus detection as well as to show the vaccination efficacy. Previous studies, such as COVIDX-Net, VGG-19, and COVID-Net, have achieved promising results. However, many rely solely on accuracy and lack interpretability. A study [16] has presented an assessment of the vaccination efficacy in vaccinated and unvaccinated COVID-19 patients. The experimental results depicted that, in comparison to the vaccinated group, lung parenchymal involvement is more prevalent among the unvaccinated participants. In addition, a CNN-COVID has been introduced in [17] to classify different datasets repositories, such as COVID-19 and BIMCV COVID-19+ of X-ray patients' images.

A mix of CNN and wavelets has been introduced in [18] to diagnose the image of lung X-rays. The experimental results were visualized by the gradient class activation map technique to assess the performance of the model. On the other hand, a CNN model has been presented in [19] to diagnose COVID using X-ray images; the experimental results depicted two categories: normal and COVID-19. While [20] has proposed three binary decision trees, each of which was trained by CNN layers and X-ray chest images, which are used as input CNN layers. The results have shown that the first decision tree classifies normal and abnormal images, while the second decision tree detects the tuberculosis indication in abnormal images, and the third decision tree detects the COVID-19 indication. Similarly, a deep learning-based X-ray chest image classification has been proposed in [21] to distinguish unique patterns in unseen images that indicate COVID-19 infection.

## 3. PROPOSED METHOD

The proposed model is obtained on classified X-ray chest images into three categories: unaffected by COVID-19, normal, and affected by the virus. First, the processing of datasets of X-ray chest images starts by preprocessing all X-ray images to eliminate undesired regions to get the lung images ready for training. Then, by training each X-ray chest image of the dataset using four CNNs (4CNN), each of which has a different architecture. The suggested model is depicted in Fig. 1.

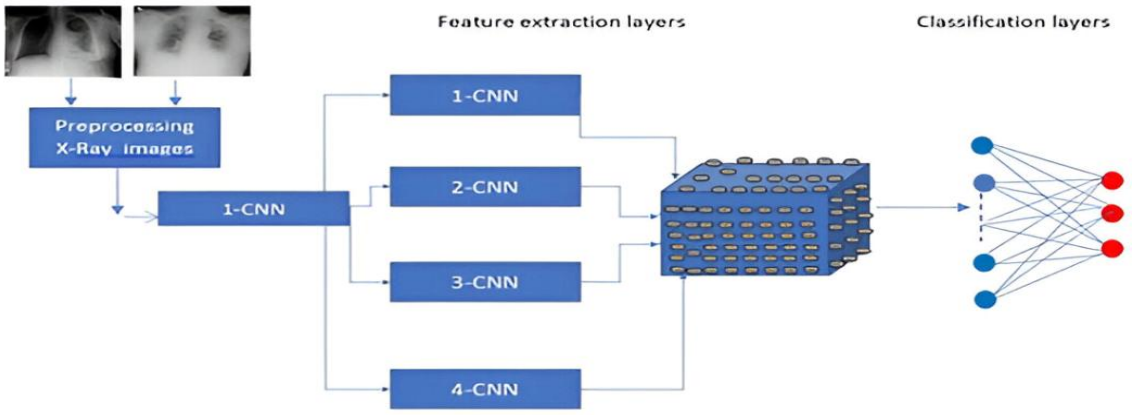


**Fig.1.** Proposed model for X-ray image classification into unaffected by COVID-19, normal, and affected.

### 3.1 DATASET DESCRIPTION

The aim of this work is to detect the lung status based on the X-ray scan and to classify the patient into vaccinated, unvaccinated, or unaffected by COVID-19. The most critical aspect of the study is to acquire high performance from the CNN model, for which a quality dataset is required. We used different lung cases from the COVID-19 dataset shown in [22], ranging from normal lung, affected by COVID-19, and unaffected by the virus, for the vaccinated patients. The initial observations have shown that severe symptoms of the virus could destroy the lungs, mainly when the patient was not vaccinated, while most of the unaffected patients were vaccinated. Figure 2 shows the various classes of X-ray images, while Table 1 shows the utilized dataset [23].

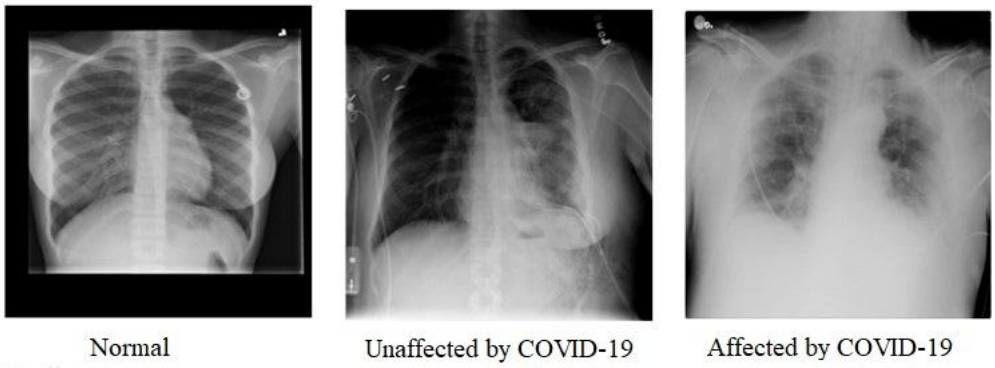


**Fig.2.** Various X-ray images for unaffected, unvaccinated, and vaccinated lung images.

**Table 1.** X-ray chest images dataset.

| Label | Training count | Validation count |
|---|---|---|
| non-COVID abnormal | 11000 | 6420 |
| Normal | 2000 | 911 |
| COVID-19 infected | 70000 | 3489 |

### 3.2 PREPROCESSING

The X-ray chest images are collected from multiple datasets in raw form. Each X-ray chest image is then preprocessed to eliminate the undesired regions, such as the upper lungs and left and right sides of the lungs, using spatial transformation. Figure 3 illustrates the filtration example by reducing the size of the X-ray image from 299x299 to 201x270.

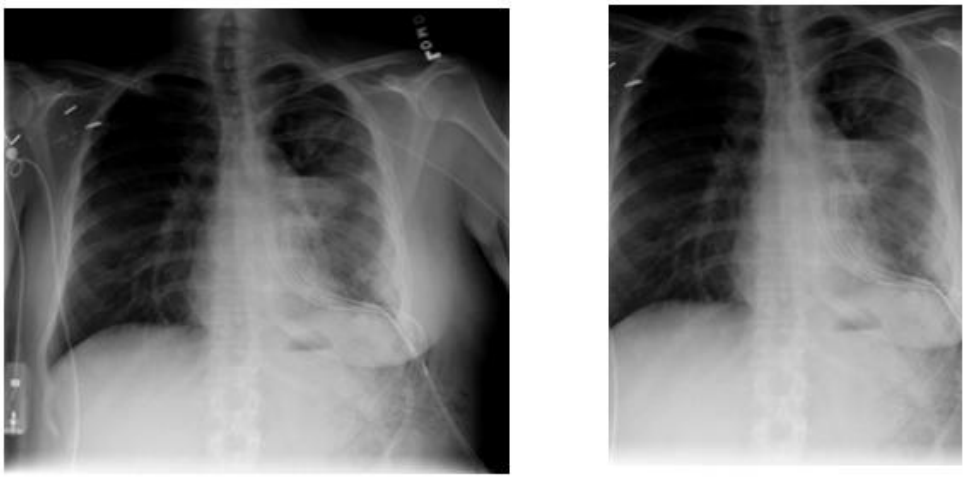


**Fig.3.** preprocessing x-ray image (a) unprocessed, (b) processed.

The proposed CNN's architecture consists of four connected layers as feature extractors. The output of the first CNN is forwarded to the second, third, and fourth CNN layers, which are then connected to classification layers. The architecture of CNNs used in the proposed work is shown in Figure 4.

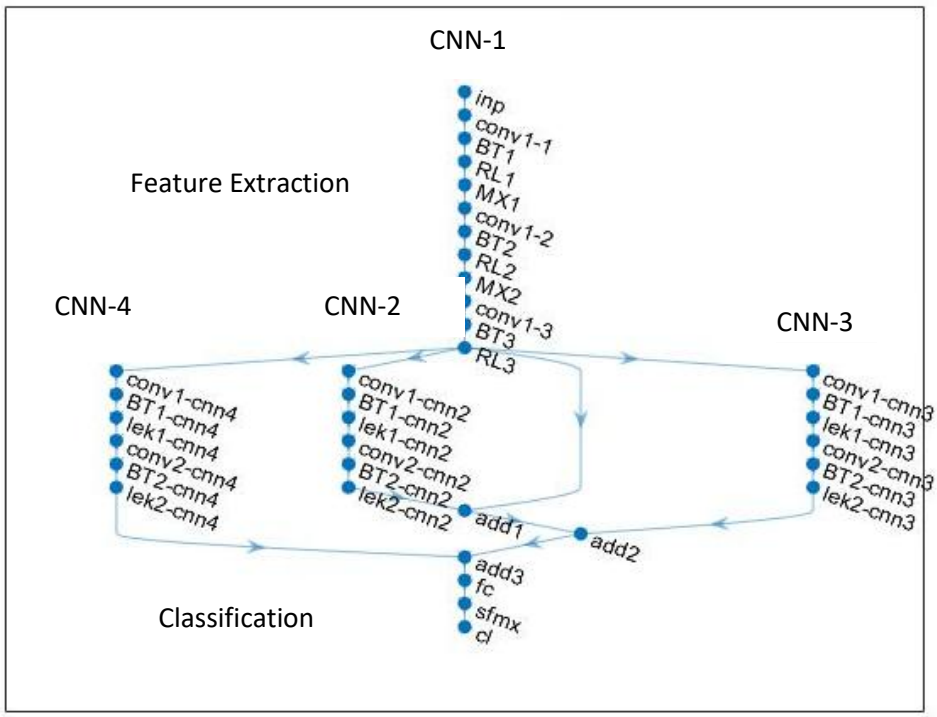


**Fig.4**. The 4CNN architecture.

To classify the X-ray images into affected, unaffected by the virus, and normal, the aforementioned CNN architecture shown in Figure 4 was used, by convolving X-ray images using kernels to build feature maps. Kernel weights in the feature map connect units to previous layers, and these weights are changed during training using the backpropagation technique. The convolutional layer only had to learn a modest number of weights because all units utilized the same

kernels. The following components have been used together in a CNN to achieve the categorization of the three classes above.

i. Rectified Linear Unit (ReLU) layer: Each element of the input is subjected to a threshold operation by a ReLU layer, with any value less than zero set to zero, as shown in

$$F(x) = \begin{Bmatrix} x, x \geq 0 \\ 0, x < 0 \end{Bmatrix} \quad (1)$$

ii. A leaky ReLU layer: Conducts a threshold operation, which multiplies any input value less than zero by a constant scalar such that,

$$F(x) = \begin{Bmatrix} x, x \geq 0 \\ constant.x, x < 0 \end{Bmatrix} \quad (2)$$

iii. Max-pooling: This layer connects spatially adjacent feature maps for maximum pooling. To preserve the position information, overlapping pools with a pool size of 3x3 receptive fields and 2x2 stride have been used, as shown in

$$S(T * F)_{i,j} = \sum\sum T(x,y)F(i - m, j - n)\, x\, y \quad (3)$$

Where $T$ is a 2-dimensional array representing the X-ray chest image, and $F$ is a kernel convolution. A fully connected layer multiplies all three inputs from CNNs by weights and adds the bias, as shown in

$$CNNs = w\sum(x,y,z) + b \quad (4)$$

where *CNNs* is the proposed CNNs architecture, $w$ is the weight, ($x,y,z$) are three inputs from CNNs, respectively, and $b$ is the bias. Table 2 lists the parameters and corresponding values used for the proposed CNN architecture.

**Table 2.** 3CNN's architecture and parameter setting in the proposed study to classify among vaccinated, unvaccinated, and unaffected.

| *Layers* | *Input layer* | *# of filters* | *weights* | *Bias* | *Offset* | *scale* |
|---|---|---|---|---|---|---|
| *Image Input* | 270x201 | 1 | 3x3x1x8 | | | |
| *Convolution* | 270x201 | 8 | | 1x1x8 | 1x1x8 | 1x1x8 |
| *Batch normalization* | 270x201 | 8 | | | 1x1x8 | 1x1x8 |
| *Relu* | 270x201 | 8 | - | - | - | - |
| *Max pooling* | 135x100 | 8 | - | - | - | - |
| *Convolution* | 135x100 | 16 | 3x3x8x16 | 1x1x16 | 1x1x16 | 1x1x16 |
| *Batch normalization* | 135x100 | 16 | | | 1x1x16 | 1x1x16 |
| *Relu* | 135x100 | 16 | - | - | - | - |
| *Max pooling* | 67x50 | 16 | - | - | - | - |
| *Convolution* | 67x50 | 16 | 3x3x16x16 | 1x1x16 | 1x1x16 | 1x1x16 |
| *Batch normalization* | 67x50 | 16 | | | 1x1x16 | 1x1x16 |
| *Relu* | 67x50 | 16 | | | | |
| *Convolution* | 67x50 | 16 | 3x3x16x16 | 1x1x16 | 1x1x16 | 1x1x16 |
| *Batch Normalization* | 67x50 | 16 | | | 1x1x16 | 1x1x16 |
| *Leaky Relu* | 67x50 | 16 | - | - | - | - |

| | | | | | | |
|---|---|---|---|---|---|---|
| *Convolution* | 67x50 | 16 | 3x3x16x16 | 1x1x16 | 1x1x16 | 1x1x16 |
| *Batch normalization* | 67x50 | 16 | | | 1x1x16 | 1x1x16 |
| *Leaky Relu* | 67x50 | 16 | - | - | - | - |
| *Addition* | 67x50 | 16 | - | - | - | - |
| *Convolution* | 67x50 | 16 | 3x3x16x16 | 1x1x16 | 1x1x16 | 1x1x16 |
| *Batch normalization* | 67x50 | 16 | | | 1x1x16 | 1x1x16 |
| *Leaky Relu* | 67x50 | 16 | - | - | - | - |
| *Addition* | 67x50 | 16 | - | - | - | - |
| *Convolution* | 67x50 | 16 | 3x3x16x16 | 1x1x16 | 1x1x16 | 1x1x16 |
| *Batch normalization* | 67x50 | 16 | | | 1x1x16 | 1x1x16 |
| *Leaky Relu* | 67x50 | 16 | - | - | - | - |
| *Addition* | 67x50 | 16 | - | - | - | |
| *Fully connected* | | | 3x53600 | 3x1 | - | - |
| *Softmax* | | - | - | - | - | - |
| *Classification output* | | - | - | - | - | - |

## 4. RESULTS AND DISCUSSION

This section performs validation and assessments of our approach to verify the proposed model using MATLAB 2019a. The data was divided into two segments: 50% for training, and 50% for validation, and testing. Figure 3 shows a preprocessed X-ray image for our three classes that are unaffected by COVID-19, normal, and affected by the virus, by eliminating the undesired region of the X-ray image. We have used a varying number of X-ray image datasets to train and validate the performance of the proposed 4CNNs. Figure 5 shows the effect of preprocessing on the dataset of X-ray images. The proposed model achieves 92% accuracy, confirming robust performance. Compute Precision, recall, F1-score, specificity, etc. Table 3 illustrates the metrics of 4CNN model. The sensitivity values were high across all classes, with scores of 0.8297, 0.7915, and 0.8847, resulting in a macro-average sensitivity of 0.8353. This demonstrates the CNN's strong ability to correctly identify positive samples. The micro-average sensitivity was 0.8222, matching the overall accuracy. For specificity, the CNN showed robust negative class detection, achieving values of 0.8542, 0.9005, and 0.9394 across the classes. The macro-average specificity was 0.8980, and the micro-average specificity was 0.9111, indicating effective discrimination of negative samples. These results demonstrate that the 4CNN model provides reliable and balanced performance with strong sensitivity and specificity, making it suitable for multi-class classification tasks despite variations in class-level precision. A Comparative analysis shows competitive results against existing methods with added interpretability.

**Table.3** The metrics of 4CNN model

| name | classes | | | macroAVG | microAVG |
|---|---|---|---|---|---|
| true_positive | 5967 | 2384 | 545 | 2965.3 | 2965.3 |
| false_positive | 1225 | 628 | 71 | 641.33 | 641.33 |
| false_negative | 3099 | 7031 | 9586 | 6572 | 6572 |
| true_negative | 3099 | 7031 | 9586 | 6572 | 6572 |
| precision | 0.91857 | 0.75419 | 0.46862 | 0.71379 | 0.82218 |
| sensitivity | 0.82967 | 0.7915 | 0.88474 | 0.8353 | 0.82218 |
| specificity | 0.85419 | 0.90049 | 0.93944 | 0.89804 | 0.91109 |
| accuracy | 0.82218 | 0.82218 | 0.82218 | 0.82218 | 0.82218 |
| F-measure | 0.87186 | 0.7724 | 0.6127 | 0.75232 | 0.82218 |

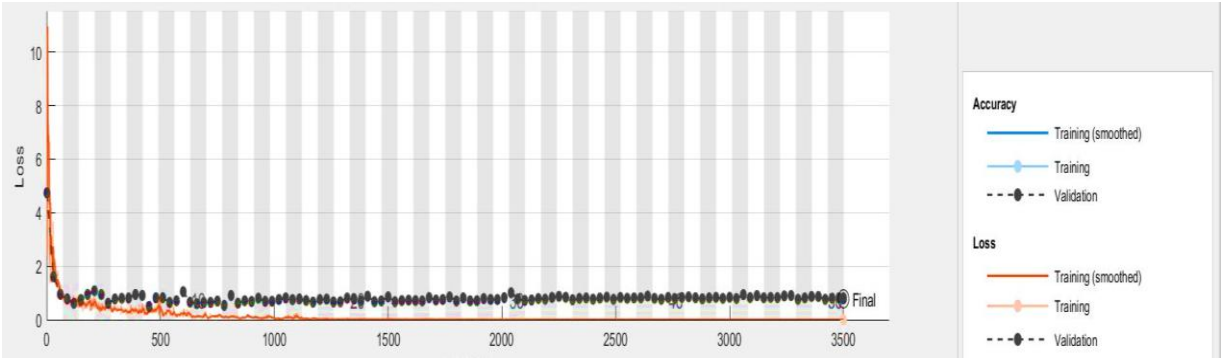


**Fig. 5:** Preprocessing dataset of X-ray chest images, black line processed data, while red unprocessed data.

Figure 6 shows a confusion matrix for unseen validation data. It can be noticed that a high accuracy of 92.0% is achieved for the non-COVID abnormal 'unaffected' class. In addition, Table 4 illustrates a comparison between the results of the proposed method and those of others that acquired different state-of-the-art methods. COVID-19 detection based on COVIDX-Net [23] had a lower assessment value. While [24] and [25] are based on the distinct architecture of the state of the art (VGG-19 and COVID-Net), respectively, with a small number of images as a dataset.

**Table 4** Comparison between different methods of the state of the art

| ***Author*** | **Method** | **Dataset** | | | **Assessment** |
|---|---|---|---|---|---|
| *Ezz et al.[23]* | COVIDX-Net | 25 COVID-19 positive | | | 90% |
| *Ioannis et al.[24]* | VGG-19 | 224 COVID-19 positive | | | 93.48% |
| *Hayden et al.[25]* | COVID-Net | 53 COVID-19 positive and 5526 COVID-19 negatives | | | 92.4% |
| *The proposed-method* | Proposed model | *Label* | *Training count* | *Validation count* | 92% |
| | | Unaffected by COVID-19 | 11000 | 6420 | |
| | | *Normal* | 2000 | 911 | |
| | | Affected by COVID-19 | 70000 | 3489 | |

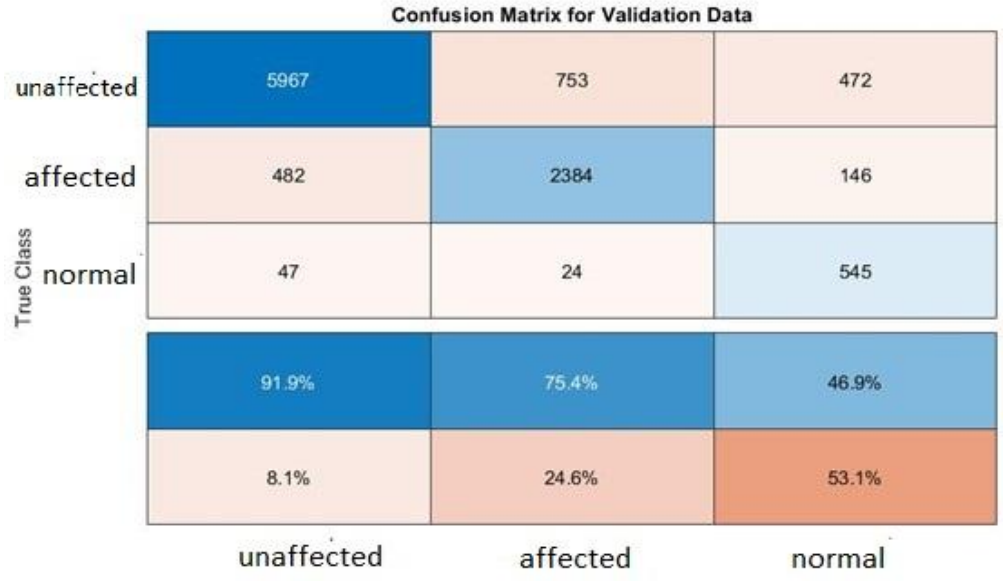


**Fig. 6.** Confusion matrix for unseen validation

## 5. CONCLUSION

To conclude, many modern applications of COVID-19 detection have sprung as a result of their critical role in classifying patient lungs into unaffected by COVID-19, normal, and affected by the virus. In this work, a new classification model utilizing X-ray images comprising human lungs was proposed. It utilizes 4 CNNs architecture that occurs in two stages and two corresponding phases. In the first phase, preprocessing of the raw X-ray chest images is performed to acquire the lung area. In the second phase, training of the deep learning model is performed over cleaned X-ray chest images. The proposed model is capable of classifying the unseen image instances into three classes: unaffected by COVID-19, normal, and affected by the virus. The proposed model is validated over unseen instances, producing an overall accuracy of 92%. Finally, it is possible to further improve the new architecture and to increase the accuracy by generalizing the data through gathering more data from different countries, including Iraq, the UK, and the UAE (according to the COVID-19 dataset used), as well as the utilization of deep transfer learning for the analysis.

## References

[1] N. M. Moatz and S. A. Yousif, "COVID-19 detection via blood tests using an automated machine learning tool (Auto-Sklearn)," *Iraqi Journal of Science*, vol. 64, no. 11, pp. 6013–6024, 2023.

[2] N. Khasawneh, M. Fraiwan, L. Fraiwan, B. Khassawneh, and A. Ibnian, "Detection of COVID-19 from chest X-ray images using deep convolutional neural networks," *Sensors*, vol. 21, no. 17, p. 5940, 2021.

[3] M. Helal Uddin *et al.*, "Detecting COVID-19 status using chest X-ray images and symptoms analysis by own developed mathematical model: A model development and analysis approach," *COVID*, vol. 2, no. 2, pp. 117–137, 2022, doi: 10.3390/covid2020009.

[4] M. Islam *et al.*, "Diagnosis of COVID-19 from X-rays using combined CNN–RNN architecture with transfer learning," *Bench Council Transactions on Benchmarks, Standards and Evaluations*, vol. 2, no. 4, p. 100088, 2022.

[5] I. N. Yulita *et al.*, "Machine learning approach for new COVID-19 cases using recurrent neural networks and long-short term memory," *Iraqi Journal of Science*, vol. 64, no. 11, pp. 5887–5895, 2023.

[6] P. Mahesh *et al.*, "COVID-19 detection from chest X-ray using convolution neural networks," in *Proc. IOP Conf. Series: Materials Science and Engineering*, vol. 1804, no. 1, p. 012197, Feb. 2021.

[7] G. Jia, H.-K. Lam, and Y. Xu, "Classification of COVID-19 chest X-ray and CT images using a type of dynamic CNN modification method," *Computers in Biology and Medicine*, vol. 134, p. 104425, 2021, doi: 10.1016/j.compbiomed.2021.104425.

[8] N. S. Shadin, S. Sanjana, and N. J. Lisa, "COVID-19 diagnosis from chest X-ray images using convolutional neural network (CNN) and InceptionV3," in *Proc. Int. Conf. Information Technology (ICIT)*, 2021, pp. 799–804, doi: 10.1109/ICIT52682.2021.9491752.

[9] L. Huang, S. Ruan, and T. Denoeux, "COVID-19 classification with deep neural network and belief functions," in *Proc. 5th Int. Conf. Biological Information and Biomedical Engineering*, Hangzhou, China, 2021.

[10] M. Shorfuzzaman and M. Masud, "On the detection of COVID-19 from chest X-ray images using CNN-based transfer learning," *Computers, Materials & Continua*, vol. 64, no. 3, pp. 1359–1381, 2020.

[11] N. Khasawneh, M. Fraiwan, L. Fraiwan, B. Khassawneh, and A. Ibnian, "Detection of COVID-19 from chest X-ray images using deep convolutional neural networks," *Sensors*, vol. 21, no. 17, p. 5940, 2021.

[12] S. Podder, S. Bhattacharjee, and A. Roy, "An efficient method of detection of COVID-19 using Mask R-CNN on chest X-ray images," *AIMS Biophysics*, vol. 8, no. 3, pp. 281–290, 2021.

[13] M. G. Hussain and Y. Shiren, "Recognition of COVID-19 disease utilizing X-ray imaging of the chest using CNN," in *Proc. Int. Conf. Computing, Electronics & Communications Engineering (iCCECE)*, 2021, pp. 71–76, doi: 10.1109/iCCECE52344.2021.9534839.

[14] E. Irmak, "Implementation of convolutional neural network approach for COVID-19 disease detection," *Physiological Genomics*, vol. 52, no. 12, pp. 590–601, 2020.

[15] A. Abbas, M. M. Abdelsamea, and M. M. Gaber, "Classification of COVID-19 in chest X-ray images using DeTraC deep convolutional neural network," *Applied Intelligence*, vol. 52, no. 12, pp. 854–864, 2020.

[16] V. Granata *et al.*, "Imaging severity COVID-19 assessment in vaccinated and unvaccinated patients: Comparison of the different variants in a high-volume Italian reference center," *Journal of Personalized Medicine*, vol. 12, no. 6, p. 955, 2022.

[17] P. M. De Sousa *et al.*, "COVID-19 classification in X-ray chest images using a new convolutional neural network: CNN-COVID," *Research on Biomedical Engineering*, vol. 38, pp. 1–11, 2021, doi: 10.1007/s42600-020-00120-5.

[18] S. Gunasekaran *et al.*, "Wavelet-based CNN for diagnosis of COVID-19 using chest X-ray," in *Proc. 1st Int. Conf. Circuit, Signal, Systems and Securities*, 2021, p. 012015, doi: 10.1088/1757-899X/1084/1/012015.

[19] R. M. James and M. R. Arief, "Classification of X-ray COVID-19 image using convolutional neural network," in *Proc. 2nd Int. Conf. Cybernetics and Intelligent System (ICORIS)*, Manado, Indonesia, 2020, pp. 1–6, doi: 10.1109/ICORIS50180.2020.9320828.

[20] S. H. Yoo *et al.*, "Deep learning-based decision-tree classifier for COVID-19 diagnosis from chest X-ray imaging," *Frontiers in Medicine*, vol. 7, p. 427, 2020, doi: 10.3389/fmed.2020.00427.

[21] C. E. Belman-López, "Detection of COVID-19 and other pneumonia cases using convolutional neural networks and X-ray images," *Ingeniería e Investigación*, vol. 42, no. 1, 2022.

[22] T. Rahman, "COVID-19 Radiography Database," Kaggle, [Online]. Available: https://www.kaggle.com/datasets/tawsifurrahman/covid19-radiography-database

[23] "COVID-19 Radiography Database: COVID-19 chest X-ray images and lung masks database," Kaggle, Accessed: Jul. 13, 2023. [Online]. Available: https://www.kaggle.com/datasets/tawsifurrahman/covid19-radiography-database

[24] E. E.-D. Hemdan, M. A. Shouman, and M. E. Karar, "COVIDX-Net: A framework of deep learning classifiers to diagnose COVID-19 in X-ray images," *arXiv preprint* arXiv:2003.11055, 2020, doi: 10.48550/arXiv.2003.11055.

[25] I. D. Apostolopoulos and T. A. Mpesiana, "COVID-19: Automatic detection from X-ray images utilizing transfer learning with convolutional neural networks," *Physical and Engineering Sciences in Medicine*, vol. 43, pp. 635–640, 2020.

[26] H. Gunraj, L. Wang, and A. Wong, "COVIDNet-CT: A tailored deep convolutional neural network design for detection of COVID-19 cases from chest CT images," *Frontiers in Medicine*, vol. 7, 2020, doi: 10.3389/fmed.2020.608525.